Received: 17 July 2020 | Revised: 8 December 2020 | Accepted: 15 February 2021

DOI: 10.1049/rpg2.12155

IET Renewable Power Generation

The Institution of Engineering and Technology WILEY

ORIGINAL RESEARCH PAPER

# Performance assessment of a novel power generation system

**Narayanan Shankar Ganesh**[1] | **Gunasekaran Uma Maheswari**[2] | **Tangellapalli Srinivas**[3] | **Bale Viswanadha Reddy**[4]

[1] Department of Mechanical Engineering, Kingston Engineering College, Vellore, Tamil Nadu 632059, India

[2] Department of Computer Applications, School of Information Technology and Engineering, Vellore Institute of Technology, Vellore, Tamil Nadu 632014, India

[3] Department of Mechanical Engineering, Dr. B.R. Ambedkar National Institute of Technology, Jalandhar, Punjab 144001, India

[4] Department of Mechanical and Manufacturing Engineering, Faculty of Engineering and Applied Science, Ontario Tech University (UOIT), Oshawa ONL1H 7K4, Canada

**Correspondence**
N. Shankar Ganesh, Department of Mechanical Engineering, Kingston Engineering College, Vellore, Tamil Nadu, 632059, India.
Email: nshankar_g@rediffmail.com

**Abstract**

This paper introduces a novel power generation system using solar energy as a heat source. The proposed cycle incorporates heat sources from two solar collectors for the effective utilisation of heat energy. To aid the performance of the proposed system, the turbine flow rate is increased with the specific heater arrangements. Energy and exergy balances of the novel system were generated using Python software. The investigation of the present system was evaluated with high sink temperature. Turbine inlet concentration, turbine inlet pressure, $HE_4$ outlet temperature from the turbine, condenser concentration of ammonia, isentropic efficiency of the turbine and pressure ratio are the design variables considered for the exergy and thermoeconomic investigation. The energy and exergy analyses resulted in suitable design variables to optimise the performance. The optimum Kalina cycle efficiency, solar plant efficiency, exergy efficiency and network output were determined to be 18.51%, 8.28%, 34.51% and 295.24 kW, respectively. Among the components involved in the system, the mixers account for the highest exergy destruction followed by the turbine. The cycle performance can be improved by reducing the exergy destruction rate. The thermal efficiency is maximised by the turbine inlet pressure and temperature. Moreover, a higher relative cost difference has resulted in heat exchanger 5 and pump 2.

## 1 | INTRODUCTION

The growth in population results in increased energy consumption. Energy demand in the near future is unpredictable with this high world population. To meet out the energy demand, a substitute for the conventional energy generation is required. Hence, more power generation systems that focus on renewable energy sources can solve this global challenge. There is a need for the development of power generation systems utilising low- to medium-temperature heat sources, as opposed to high-temperature sources. Renewable energy sources are considered the best replacements for fossil fuels in multigeneration systems [1].

Ghaebi et al. [2–4] claimed the majority of the exergy destruction rate of the novel cascade Kalina system occurs in the second heat exchanger, condenser (CND), vapour generator. Dhahad et al. [5] proposed that the sum unit cost of the products are influenced by low temperature heat recovery (LTHS) inlet temperature, absorber temperature, condenser temperature and LTHS temperature at the heat exchanger outlet. Exergy analysis of a modified Kalina cycle (KC) was proposed by Mokarram and Mosaffa [6]. In their modified KC, the throttle valve was replaced with a two-phase expander. The maximum exergy destruction was recorded in the evaporator at the optimised conditions. A thermoeconomic investigation of a combined Brayton–Rankine–Kalina triple power cycle was performed by Singh and Kaushik [7]. The relative cost difference in the recuperator and evaporator was highest with the Kalina bottoming cycle. An exergoeconomic examination was carried out using the tool SPECO, which identifies cost efficiency. Ghaebi et al. [8] proposed a low-temperature KC with liquefied natural gas as a combined power and cooling cycle. The heat exchanger and throttling valve have high exergy losses. Also, the first law efficiency is high at higher ammonia concentration, while the second law efficiency maximises at lower ammonia concentration. Sun et al. [9] assessed exergetically the performance of a KCS-11 with an additional superheater in a low-grade thermal energy conversion system. The system performance was more concerned with the exergy losses in the turbine and condenser.

In a study conducted by Abdolalipouradl et al. [10], an exergoeconomic analysis of an integrated transcritical CO2 and KCS-11 cycle was conducted using two wellheads, which resulted in high performance in energy and exergy perspectives. Mehrpooya and Mousavi [11] presented an advanced exergy and exergoeconomic investigation on a solar-driven KC using the Aspen Plus simulation tool. The exergy destruction of the heater was high. The highest and lowest exergy destruction cost rate determined from the advanced exergy analysis occurred at the absorber and pump, respectively. Shokati et al. [12–14] examined the absorption refrigeration/Kalina cogeneration cycle. It was observed that the boiler and low-pressure absorber resulted in high exergy destruction and capital investment cost rates. The shortest payback period occurred with the Simple Absorption Refrigeration/KC. Fiaschi et al. [15] compared the organic Rankine cycle (ORC) with various working fluids and the KC, both thermodynamically and exergoeconomically at medium- and low-temperature applications. The ORC using R1233zd€ claimed superior exergoeconomic performance at medium-temperature applications, whereas the KC proved the best performance at low-temperature applications. A comparison of two KCs, Kalina cooling-power cycle (KPCC) and Kalina LiBr-H2O absorption chiller cycle (KLACC), was made by Rashidi and Yoo [16]. The total exergy destruction of KLACC was larger than KPCC, as the condenser and second flash tank preheater resulted in major losses. Mahmoudi et al. [17] combined a KC with a gas turbine modular helium reactor and concluded that the helium mass flow rate was reduced with the combined system favouring a size reduction of the system. As per the literature and by examination of other literature reviews, few exergoeconomic analyses of power generation systems suitable for medium-temperature applications have been conducted. In this work, a novel Kalina power generation cycle suitable for generating power from solar energy is presented and examined at high sink temperature. The main goals of the present study are listed below:

1. Investigation of a novel ammonia-water mixture binary system recovering waste heat from medium-temperature sources.
2. Parametric investigation of the system using Python code.
3. Evaluation of the system using second law analysis.
4. Comparison of the overall system performance with the addition of solar collectors.
5. Investigation of the system for hot sink conditions.

## 2 | NOVEL KALINA POWER GENERATION SYSTEM

Figure 1 represents the renewable energy-headed power generation system driven by heat sources suitable for medium-temperature applications. An ammonia-water mixture is the working fluid in the cycle. The extension of the Rankine cycle reveals the basic concept of the KC using a binary component mixture as the working fluid [18]. The proposed solar collector heating Kalina system is shown in Figure 1. Along with the conventional Kalina configuration components, additional heat exchangers for better heat recovery from the two solar collector heat energy are included in the present system.

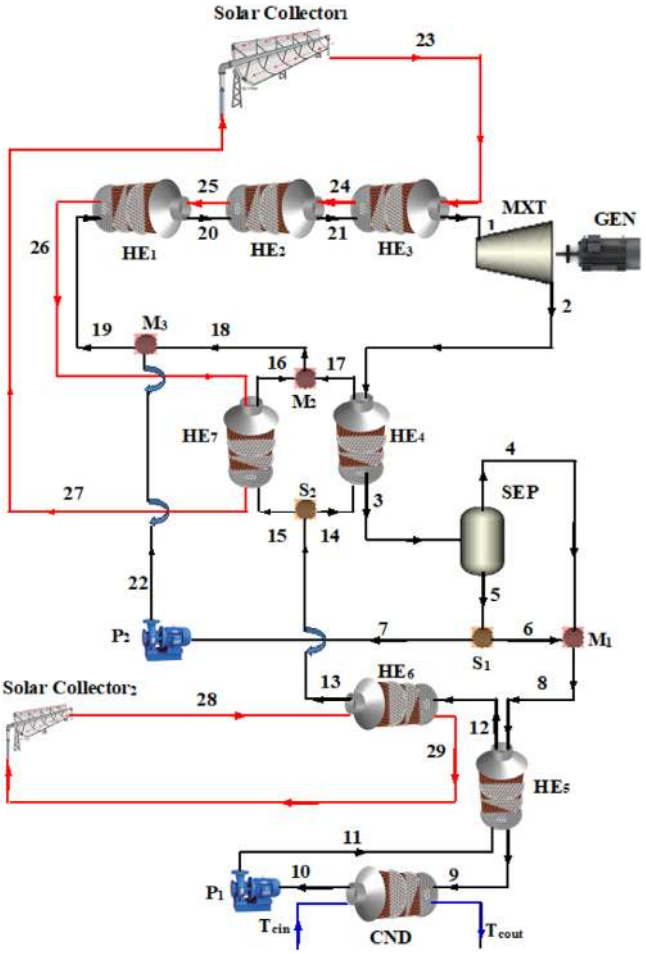


**FIGURE 1** Novel Kalina power generation system suitable for medium temperature heat recovery

In the conventional KC proposed by Ganesh and Srinivas [19] with a single solar collector, the heat is efficiently recovered in the heat exchangers. In the system proposed in this study, the additional solar collector provides more heat recovery in the heat exchanger $HE_6$. To condense the working fluid at the low pressure in the condenser, the liquid concentration of ammonia-water mixture from the separator (state 5) is combined with the vapour concentration of the mixture (state 4). A portion of the liquid concentration of the mixture (state 7) is combined with the inlet stream (state 19) of the heat exchanger ($HE_1$). With the two streams mixing, an additional mass flow rate to the turbine is produced with 1 kg/s of flow from the condenser. With the additional solar collector, the system results in higher energy and exergy performance on a cost basis. The entire system uses a mixture as working fluid rather than a single component; hence, the irreversibility in the boiling and condensing units are minimised, compared to the conventional Rankine cycle. The temperature difference between the hot source and working fluid is reduced owing to the non-isothermal nature of the zeotropic mixture.

The molecular weight of ammonia and water are nearly equal, leading to the use of the turbine of the Rankine system in the proposed system. The system uses two pumps to circulate the condensing fluid to the heat exchangers $HE_4$ and $HE_7$ and to divert the recirculating ammonia lean liquid mixture to the heat exchanger $HE_1$. As an alternative to the solar collectors, the proposed system uses the waste heat from an internal combustion engine fuelled with a diesel and algae oil blend, resulting in identical performance. The separator is located below the turbine favouring a high inlet concentration. The KC is generally suitable for low-temperature heat recovery applications and considered comparable to the ORC. Most power generation cycles are proposed for low- and high-temperature heat recovery applications; hence, in the present work, medium-temperature heat recovery application was the focus. The advanced medium-temperature heat recovery applications had better performance and less expense, compared to low-temperature heat recovery applications. The liquid and vapour concentration at the separator was evaluated using bubble and dew point temperatures [20]. The thermodynamic properties of the binary mixture at every state point were evaluated with a mass and energy balance in the components through Python coding.

## 3 | FIRST AND SECOND LAW ANALYSIS

### 3.1 | Assumptions [10, 19]

The following assumptions apply to the present study:

1. The components of the Kalina system operate in steady-state conditions.
2. The changes in kinetic and potential energies are negligible.
3. Pressure drops and pipeline heat losses are negligible.
4. The pumps and turbine operate isentropically.
5. The mechanical efficiencies of the turbine and pump are 96%.
6. The pressure and temperature at atmospheric conditions are 1.013 bar and 25°C, respectively.
7. In superheater $HE_3$, 25°C is the terminal temperature difference.
8. At the condenser, there is a 5°C pinch point temperature difference.
9. An isenthalpic process occurs at the throttle valve.
10. The condensate is saturated liquid at the condenser.

### 3.2 | First law analysis

Using the first law analysis, the energy performance of the novel Kalina system was assessed.

The KC efficiency of the system was derived as the output to input [18].

$$\eta_{KC} = \frac{\dot{m}_1(h_1 - h_2) - [\dot{m}_{11}(h_{11} - h_{10}) + \dot{m}_{22}(h_{22} - h_7)]}{\dot{m}_1(h_1 - h_{31}) + \dot{m}_{21}(h_{21} - h_{20}) + \dot{m}_{20}(h_{20} - h_{19}) + \dot{m}_{14}(h_{16} - h_{15})} \times 100 \quad (1)$$

The parabolic trough collector design features are outlined in the literature [21].

Solar plant efficiency

$$\eta_{Plant} = \frac{W_{net}}{R_g \times A_{c,tot}} \times 100 \quad (2)$$

$A_{c,tot}$ is the total area of collection.

### 3.3 | Exergy analysis

Exergy is the maximum theoretical useful work obtained upon interacting with the system to equilibrium. At equilibrium, the maximum useful output attained theoretically by a system is determined in exergy analysis [2]. In thermal systems, the specific exergy of the components is evaluated with the summation of physical and chemical components.

Physical and chemical exergy rates for each state points of the cycle is given by [10, 1]:

$$\dot{E}x_{ph,i} = \dot{m}(h - h_0) - T_0(s - s_0) \quad (3)$$

$$\dot{E}x_{ch,i} = m\left(\left[\frac{ex^0_{ch,NH_3}}{M_{NH_3}}\right]x + \left[\frac{ex^0_{ch,H_2O}}{M_{H_2O}}\right](1 - x)\right) \quad (4)$$

where $M$ is the molecular weight of the individual components ($M_{NH3} = 17$, $M_{H2O} = 18$), $\dot{E}x_{ph,i}$ is physical exergy, $\dot{E}x_{ch,i}$ is chemical exergy and 0 refers to the atmospheric condition [1].

The total exergy for the individual components is defined in Equation (5).

$$\dot{E}x_{total,i} = \dot{E}x_{ph,i} + \dot{E}x_{ch,i} \quad (5)$$

The useful concepts introduced in exergy analysis are fuel and product. The desired results produced are the product and the spent resources to produce the product are the fuel. These concepts are expressed as exergy destruction rate. The exergy destruction and the exergetic efficiency for the individual components are specified as

$$\dot{E}x_{D,i} = \dot{E}x_{F,i} - \dot{E}x_{P,i} \quad (6)$$

The maximum theoretical work required for producing the ideal work is called fuel exergy [2]. Fuel exergy and product exergy are essential in evaluating exergoeconomic analysis [22]. The exergetic efficiency is specified in Equation (7):

$$\varepsilon_i = \frac{\dot{E}x_{P,i}}{\dot{E}x_{F,i}} 100 \quad (7)$$

The exergy destruction ratio is as follows in Equation (8):

$$y_{D,i} = \frac{I_{D,i}}{I_{D,Total}} \quad (8)$$

### 3.4 | Thermoeconomic analysis

Thermoeconomic analysis combines exergy and economic principles in evaluating the performance of power generation systems [1]. Moreover, a cost-effective system can be with the result of a thermoeconomic evaluation. The cost-based balance and auxiliary equations are derived in carrying out the thermoeconomic analysis for the components. The summation of the total fuel cost rate $\dot{C}_{F,tot}$, total capital investment cost rate $\dot{Z}^{CI}$ and the total operating and maintenance cost rate $\dot{Z}^{OM}$ equals the total product cost rate $\dot{C}_{P,tot}$ of the system and is expressed to balance the cost in a system [23].

$$\dot{C}_{P,tot} = \dot{C}_{F,tot} + \dot{Z}^{CI}_{tot} + \dot{Z}^{OM}_{tot} \tag{9}$$

The total cost rate of the $i$th component is the summation of the capital investment cost rate ($\dot{Z}^{CI}$) and operating and maintenance cost rate ($\dot{Z}^{OM}$).

$$\dot{Z}_i = \dot{Z}^{CI}_i + \dot{Z}^{OM}_i \tag{10}$$

The cost in exergy is associated with every individual exergy stream [23]. The exergy transfer rate for the inlet and outlet streams, work and heat transfer is as follows:

$$\dot{C}_{inlet} = c_{inlet}\dot{E}_{inlet} \tag{11}$$

$$\dot{C}_{exit} = c_{exit}\dot{E}_{exit} \tag{12}$$

$$C_{work} = c_{work}W \tag{13}$$

$$\dot{C}_{heat} = c_{heat}\dot{E}_{heat} \tag{14}$$

where $c_i$, $c_e$, $c_w$ and $c_q$ are the average costs per unit of exergy in dollars per gigajoule ($/GJ).

The total cost of inlet exergy streams with capital and other costs is equal to the total cost of output exergy streams for a system associated with heat work transfers [23].

$$\dot{C}_{heat,i} + \sum_{inlet}\dot{C}_{inlet,i} + \dot{Z}_i = \sum_{exit}\dot{C}_{exit,i} + \dot{C}_{work,i} \tag{15}$$

The cost rate in Equations (11) to (14) are substituted into Equation (15) as

$$c_{heat,i}\dot{E}_{heat,i} + \sum_{inlet}(c_{inlet}\dot{E}_{inlet})_i + \dot{Z}_i = \sum_{exit}(c_{exit}\dot{E}_{exit})_i + c_{work,i}W_i \tag{16}$$

The exergy destruction cost of the individual components of the novel cycle is presented in Equations (17) and (18) as below [2]:

$$\dot{C}_{D,i} = c_{P,i}\dot{E}x_{D,i}(\text{if}\dot{E}x_{F,i} = \text{constant}) \tag{17}$$

$$\dot{C}_{D,i} = c_{F,i}\dot{E}x_{D,i}(\text{if}\dot{E}x_{P,i} = \text{constant}) \tag{18}$$

where $c_{F,i}$ and $c_{P,i}$ represent the unit cost (specific) of fuel and product, respectively, of $i$th component.

Fuel exergy and product exergy of the novel cycle components are presented in Equations (19) to (30):

$$\dot{E}x_{F,HE} = \left(\dot{E}x_{HE,inlet} - \dot{E}x_{HE,outlet}\right)_{hot\ stream} \tag{19}$$

$$\dot{E}x_{F,Condenser} = \left(\dot{E}x_{Condenser,inlet} - \dot{E}x_{Condenser,outlet}\right)_{hot\ stream} \tag{20}$$

$$\dot{E}x_{F,Turbine} = \left(\dot{E}x_{Turbine,inlet} - \dot{E}x_{Turbineoutlet}\right) \tag{21}$$

$$\dot{\text{E}}\text{x}_{\text{F,Separator}} = \dot{\text{E}}\text{x}_{\text{Separator,inlet}} \tag{22}$$

$$\dot{\text{E}}\text{x}_{\text{F,Mixing chamber}} = \dot{\text{E}}\text{x}_{\text{mixing chamber,inlet1}} + \dot{\text{E}}\text{x}_{\text{mixing chamber,inlet2}} \tag{23}$$

$$\dot{E}x_{F,Pump} = \text{Specific pump work} \tag{24}$$

$$\dot{E}x_{P,HE} = \left(\dot{E}x_{HE,outlet} - \dot{E}x_{HE,inlet}\right)_{cold\ stream} \tag{25}$$

$$\dot{E}x_{P,Condenser} = \left(\dot{E}x_{Condenser,outlet} - \dot{E}x_{Condenser,inlet}\right)_{cold\ stream} \tag{26}$$

$$\dot{E}x_{P,Turbine} = \text{Specific Turbine work} \tag{27}$$

$$\dot{E}x_{P,Separator} = \dot{E}x_{Separator,liquid} + \dot{E}x_{Separator,vapour} \tag{28}$$

$$\dot{E}x_{P,Mixingchamber} = \dot{E}x_{mixingchamber,outlet} \tag{29}$$

$$\dot{E}x_{P,Pump} = \left(\dot{E}x_{pump,outlet} - \dot{E}x_{pump,inlet}\right) \tag{30}$$

The maximum theoretical work resulted in a system to produce ideal work is obtained by evaluating the exergy destruction [2]:

$$c_{P,i} = \frac{\dot{C}_{P,i}}{\dot{E}x_{P,i}} \tag{31}$$

$$c_{F,i} = \frac{\dot{C}_{F,i}}{\dot{E}x_{F,i}} \tag{32}$$

$\dot{C}_{P,i}$ and $\dot{C}_{F,i}$ are the exergy costs of product and fuel.

The conversion of capital investment into cost rate is provided in the following equation:

$$\dot{Z}_i = CRF \times \frac{\phi_r \times 365 \times 24}{N} \times z_i \tag{33}$$

where $\dot{Z}_i$ is the cost rate of each component, $z_i$ is the purchased equipment cost of the $i$th component, $N$ is the annual amount of time in operation (7000 h), $\Phi_r$ = 1.06 [2], and CRF is the capital recovery factor,

$$CRF = \frac{k(1+k)^n}{(1+k)^n - 1} \tag{34}$$

**TABLE 1** Individual components investment cost [3, 7]

| Component | Investment cost rate ($\dot{Z}$) | Constants |
|---|---|---|
| Heat exchangers ($HE_1$, $HE_2$, $HE_4$, $HE_5$, $HE_6$, $HE_7$) | $\dot{Z}_j = Z_R(\frac{A}{A_R})^{0.6}$ | Reference cost ($Z_R$), 16,000 \$$A_R$, 100 $m^2$Overall heat transfer coefficient, (U), 0.9 kW/$m^2$ K |
| Vapour generator, $HE_3$ | $\dot{Z}_{HE3} = Z_R(\frac{A}{A_R})^{0.6}$ | Reference cost ($Z_R$), 17,500 \$$A_R$, 100 $m^2$Overall heat transfer coefficient, (U), 1.6 kW/$m^2$ K |
| Condenser (CND) | $\dot{Z}_{CND} = Z_R(\frac{A}{A_R})^{0.6}$ | Reference cost ($Z_R$), 8000 \$$A_R$, 100 $m^2$Overall heat transfer coefficient, (U), 1.1 kW/$m^2$ K |
| Turbine | $\dot{Z}_{MXT} = 4405 \times \dot{W}_{Tur}^{0.7}$ | – |
| Pump | $\dot{Z}_{Pump} = \dot{Z}_{R,Pump}(\frac{\dot{W}_{Pump}}{\dot{W}_{R,Pump}})^{m_p}(\frac{1-\eta_{is,pump}}{\eta_{is,pump}})^{n_p}$ | $Z_{R,Pump}$, 2100 \$$\dot{W}_{R,Pump}$, 10 kW$m_p = 0.26n_p = 0.5$ |

The relative cost difference $r_i$ of the system $i$th component is as below:

$$r_i = \frac{c_{P,i} - c_{F,i}}{c_{F,i}} \tag{35}$$

where the interest rate $k = 0.15$ [1], and the total operating period of the cycle $n = 20$ years [1].

The relative cost difference is a variable to assess and optimise the system component [38].

The exergoeconomic factor $f_i$ identifies the significance of the component's performance in the system.

The investment costs of individual components were assessed in determining the total investments cost of the system [7]. Table 1 summarises the investment cost of each component of the proposed system. The investment costs of the separator and mixing chamber were considered negligible [7].

The areas for the heat exchangers, vapour generator and condenser were evaluated utilising the logarithmic mean temperature difference and overall heat transfer coefficient [7].

Abbreviation: MXT is mixture turbine; SEP is separator.

Table 2 provides the cost-based balance and auxiliary equations for the entire components of the proposed cycle:

$$f_i = \frac{\dot{Z}_i}{\dot{Z}_i + \dot{C}_{D,i}} \tag{35}$$

$$Q = U_i A_i LMTD_i \tag{36}$$

## 3.5 | Validation

Since the proposed system is based on medium-temperature heat recovery, the results were compared with the literature [24, 25]. The cycle and exergy efficiencies of the present work are closely associated with the reported results as presented in Table 3.

**TABLE 2** Cost-based balance equations and auxiliary equations for individual components of the novel cycle

| Components | Cost equations | Auxiliary equations |
|---|---|---|
| $HE_1$ | $\dot{C}_{25} + \dot{C}_{19} + \dot{Z}_{HE1} = \dot{C}_{20} + \dot{C}_{26}$ | $c_{25} = c_{26}$ |
| $HE_2$ | $\dot{C}_{24} + \dot{C}_{20} + \dot{Z}_{HE2} = \dot{C}_{21} + \dot{C}_{25}$ | $c_{24} = c_{25}$ |
| $HE_3$ | $\dot{C}_{23} + \dot{C}_{21} + \dot{Z}_{HE3} = \dot{C}_1 + \dot{C}_{24}$ | $c_{23} = c_{24}$ |
| $HE_4$ | $\dot{C}_2 + \dot{C}_{14} + \dot{Z}_{HE4} = \dot{C}_3 + \dot{C}_{17}$ | $c_2 = c_3$ |
| $HE_5$ | $\dot{C}_8 + \dot{C}_{11} + \dot{Z}_{HE5} = \dot{C}_9 + \dot{C}_{12}$ | $c_8 = c_9$ |
| $HE_6$ | $\dot{C}_{28} + \dot{C}_{12} + \dot{Z}_{HE6} = \dot{C}_{29} + \dot{C}_{13}$ | $c_{28} = c_{29}$ |
| $HE_7$ | $\dot{C}_{26} + \dot{C}_{15} + \dot{Z}_{HE7} = \dot{C}_{16} + \dot{C}_{27}$ | $c_{26} = c_{27}$ |
| CND | $\dot{C}_9 + \dot{C}_{Tcin} + \dot{Z}_{CND} = \dot{C}_{10} + \dot{C}_{Tcout}$ | $c_9 = c_{10}$ |
| MXT | $\dot{C}_1 + \dot{Z}_{Tur} = \dot{C}_2 + \dot{C}_{w,Tur}$ | $c_{wTur} = c_w$ |
| SEP | $\dot{C}_3 + \dot{Z}_{SEP} = \dot{C}_4 + \dot{C}_5$ | $c_2 = c_3$ |
| M1 | $\dot{C}_4 + \dot{C}_6 + \dot{Z}_{MIX} = \dot{C}_8$ | – |
| M2 | $\dot{C}_{16} + \dot{C}_{17} + \dot{Z}_{MIX} = \dot{C}_{18}$ | – |
| M3 | $\dot{C}_{22} + \dot{C}_{18} + \dot{Z}_{MIX} = \dot{C}_{19}$ | – |
| P1 | $\dot{C}_{10} + \dot{C}_{wpump1} + \dot{Z}_{pump1} = \dot{C}_{11}$ | $c_{wpump1} = c_w$ |
| P2 | $\dot{C}_7 + \dot{C}_{wpump2} + \dot{Z}_{pump2} = \dot{C}_{22}$ | $c_{wpump2} = c_w$ |

**TABLE 3** Validation of novel Kalina cycle with References [24, 25]

| Parameter | Present work | Reference [24] | Reference [25] |
|---|---|---|---|
| Hot source temperature (°C) | 190 | 280 | 167.9 |
| High pressure (bar) | 45 | 60 | 7.5 |
| Flow rate at turbine (kg/s) | 1.48 | 1.23 | 2.83 |
| Cycle efficiency (%) | 18.51 | 20.9 | 11.24 |
| Exergy efficiency (%) | 34.51 | 41.9 | 49.37 |
| Net power (kW) | 295.24 | 495 | 782 |
| Pinch point temperature difference at $HE_3$ (°C) | 8 | 20 | 15 |

## 4 | RESULTS AND DISCUSSION

With the previously mentioned assumptions, the proposed power generation system was simulated with Python coding on energy and exergy bases [18]. A parametric investigation was performed to identify the optimised conditions. Thermoeconomic and conventional exergy analyses were conducted to assess the novel KC.

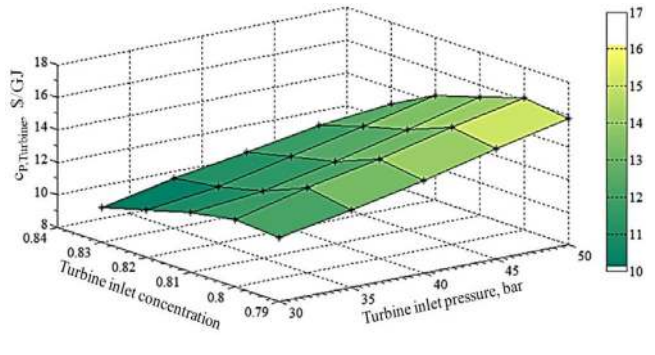


**FIGURE 2** Variation of the turbine product cost with turbine inlet pressure and turbine inlet concentration

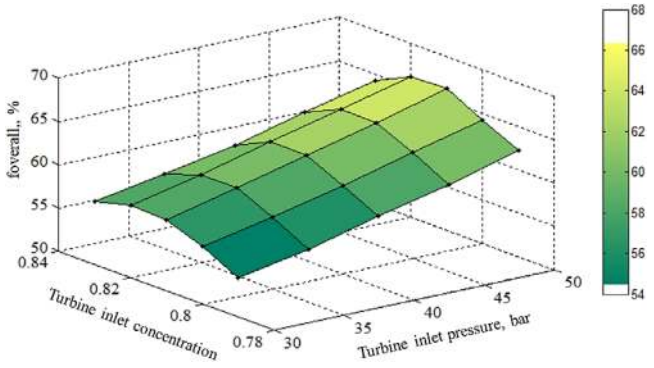


**FIGURE 3** Variation of exergoeconomic factor with turbine inlet pressure and turbine inlet concentration

## 4.1 | Parametric studies

To estimate the effects of certain variables on system performance in the energy and exergy perspectives, a detailed parametric study was performed. Turbine inlet concentration, turbine inlet pressure, $HE_4$ outlet temperature from the turbine, condenser concentration of ammonia, isentropic efficiency of the turbine and pressure ratio were the design variables considered in the performance assessment of the proposed cycle. The effects on turbine product cost are shown in Figure 2 with turbine pressure and turbine inlet concentration. Higher turbine inlet pressure yields a higher product cost of the turbine. The pressure variations of 30 to 50 bar and turbine inlet concentration of 0.79 to 0.84 were considered in evaluating the variations in the turbine cost. The higher turbine concentration also favours higher turbine cost. A higher turbine product cost results from a turbine inlet concentration of 0.8 with a value of \$16.2/GJ. At low turbine inlet concentration and pressure, the turbine product cost is a minimum value of \$9/GJ. The turbine cost rate is directly proportional to the net power generated in the cycle. The dependent functions of the turbine product cost are turbine work and the exergy of the turbine product. The unit cost of power generated in the turbine varies with the change in turbine inlet concentration, depending on the cost of power generated in the heaters.

The effect of inlet pressure variation with turbine inlet concentration is investigated based on the exergoeconomic factor as shown in Figure 3. As turbine inlet concentration increases, the exergoeconcomic factor increases to a maximum value and then declines. The capital investment cost decreases along with the total cost of exergy destruction. The $HE_3$ results in the lowest capital investment cost among the cycle components. With the combined effect of the individual component cost rate and investment cost rate of components, the exergoeconomic factor first rises and then declines as the turbine inlet concentration increases. The maximum exergoeconomic factor occurs with a high concentration of ammonia in the condenser. The optimum value of the exergoeconomic factor is 66% at turbine inlet concentration of ammonia of 0.81 and turbine inlet pressure of 45 bar.

Figure 4 presents the effects of the $HE_4$ outlet temperature and condenser concentration of ammonia on turbine product

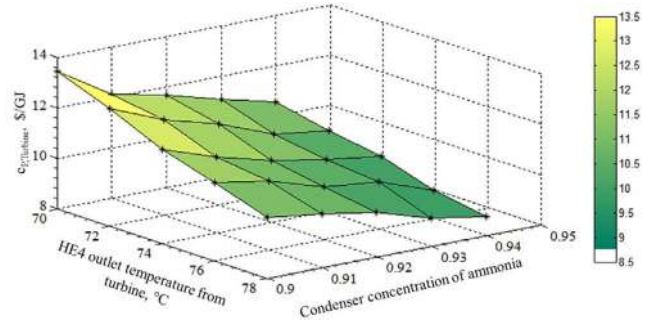


**FIGURE 4** Variation of turbine product cost with $HE_4$ outlet temperature and condenser concentration of ammonia

cost. Turbine product cost decreases with a lower condenser concentration of ammonia. Turbine product cost maximises at a higher $HE_4$ outlet temperature of 70°C and minimises at a lower $HE_4$ outlet temperature of 78°C. The lowest turbine product cost is \$8/GJ at a condenser concentration of ammonia of 0.94. A low concentration of ammonia in the condenser surpasses the specific exergy cost resulting in an increased turbine product cost. Reducing the turbine expansion will hinder the performance of the turbine and, hence, increase the turbine outlet temperature.

Figure 5 presents the effects of the pressure ratio and turbine inlet temperature on the product cost of the turbine. The total

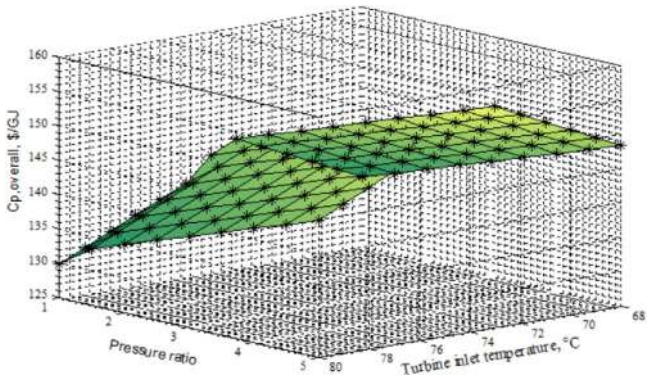


**FIGURE 5** Contribution of the proposed cycle components in $\dot{E}x_{D,i}$ parameter

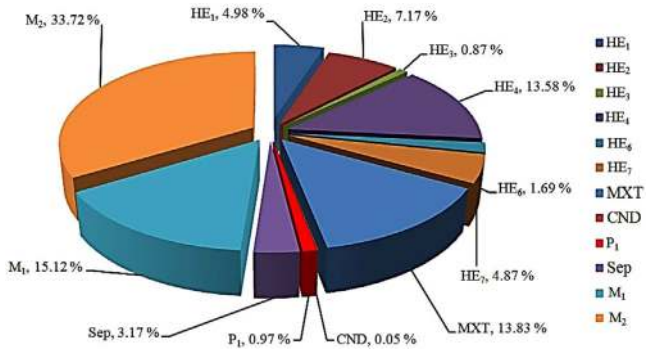


**FIGURE 6** Contribution of the proposed cycle components in $\dot{E}x_{D,i}$ parameter

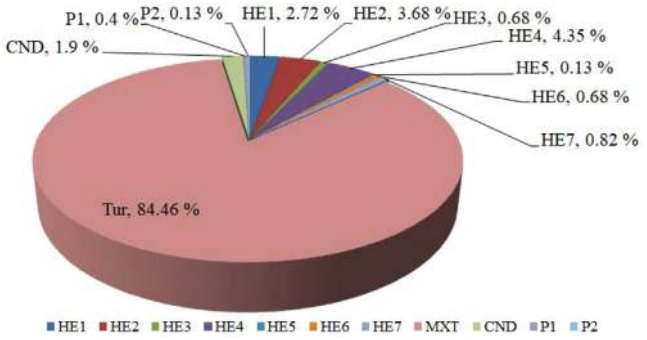


**FIGURE 7** Contribution of the proposed cycle components in $\dot{Z}_{D,i}$ parameter

product cost of the novel cycle maximises at a high-pressure ratio. Heat exchanger ($HE_5$) yields a high product cost at an increased pressure ratio followed by the turbine and condenser. The total product cost is directly proportional to the cost rate at the inlet and outlet conditions of the component and indirectly proportional to the exergy of the product. The exergy difference of $HE_5$ is low, compared to the other heat exchangers resulting in high product cost.

The cycle components of exergy destruction is presented in Figure 6. The cost rate is a function of the unit cost of fuel and exergy destruction. $M_2$ have the maximum $E_{D,i}$ in the proposed system. The percentage of $E_{D,i}$ is evaluated by dividing the individual component $E_{D,i}$ with the total $E_{D,i}$ of all components. The high and low exergy destruction rates are dependent on the $(\dot{C}_{D,i} + \dot{Z}_i)$ parameter. The component CND exhibits low exergy destruction among the components of the system. The exergy of fuel and product are nearly equal as they are dependent on the physical and chemical exergy at inlet and outlet conditions. The physical exergy of the working stream at the condenser has the smallest difference. The physical exergy of the cooling water conditions is too low at the specified parameters. Therefore, the condenser has a low exergy destruction rate. The exergy destruction rates at the inlets of the components were not the focus for performance improvement. The exergy destructions at the inlet streams of the mixing chamber are significantly less than the outlet stream, which has a high product and fuel exergy variation with a high exergy destruction rate.

The cost rates $\dot{Z}_{D,i}$ of the individual components of the proposed thermal systems are shown in Figure 7. The cost rate is directly proportional to the purchase equipment cost rate of the component. The turbine, $HE_4$ and $HE_2$ have the highest values of $\dot{Z}_{D,i}$ in the proposed system, 84.46%, 4.35% and 3.68%, respectively. The percentage cost rates for these components are 77.06%, 10.09% and 3.85%, respectively. The percentage of $\dot{Z}_{D,i}$ is evaluated by dividing the $\dot{Z}_{D,i}$ for the individual component with the total $\dot{Z}_{D,i}$ of all components.

The exergy destruction ratio with variation in isentropic efficiency of the turbine is expressed in Figure 8. High exergy destruction ratios of 39.03% and 20.77% occur at the turbine and $HE_4$, respectively. The chemical exergies of the turbine inlet and outlet are identical as they are functions of flow rate. The physical exergies at the inlet and outlet of the turbine are dependent on enthalpy and temperature. With the physical and chemical exergy variations in the turbine, the difference in fuel and product exergy values are higher than other components. Pump1 and $HE_3$ result in low exergy destruction ratio claiming 0.73% and 1.31%, respectively, at a turbine isentropic efficiency of 78%. The turbine flow rate, which increased with the proposed design, is considered as a source for improving energy performance. The high exergy destruction rate is also a result of the increased flow rate, but comparing energy and exergy performances, the influence of flow rate results in an energy boost. The turbine has a lower exergy destruction ratio at a higher isentropic efficiency, while the other components result in an adverse effect.

Figure 9 shows the result of turbine inlet concentration from 0.79 to 0.84 and turbine inlet pressure of 30 to 50 bar on the (a) KC efficiency, (b) solar plant efficiency and (c) net work output. With higher turbine inlet concentration, the net work output increases with increases in cycle efficiency and solar plant efficiency. With higher turbine inlet pressure, the turbine expansion pressure and temperature increase. The turbine work also increases with net work output and turbine inlet pressure. With an elevation in turbine inlet concentration, the total heat supplied to the system decreases with a reduction in specific work. The turbine mass flow rate increases. With these reasons, the KC and plant efficiencies improve. The KC efficiency, solar plant efficiency and network output maximise at 18.451%, 8.4% and 295.24 kW, respectively, at 45 bar turbine inlet pressure and 0.81 turbine inlet concentration. The net work will experience an adverse effect with a larger condenser temperature difference.

With the change in turbine inlet pressure, the performance variations in exergy efficiency, exergy destruction on heat exchanger $HE_3$ and total exergy destruction are presented in Figure 10. With higher turbine inlet pressure, the energy and exergy properties increase with the first and second law performances. Since the low pressure of the cycle is fixed and high pressure is varied, the higher expansion temperature at the turbine results in more specific work at the turbine. The exergy efficiency is improved with higher pressure but then declines from the high total heat supply in the heat exchangers. The exergy rate of the individual component $HE_3$ and the total exergy

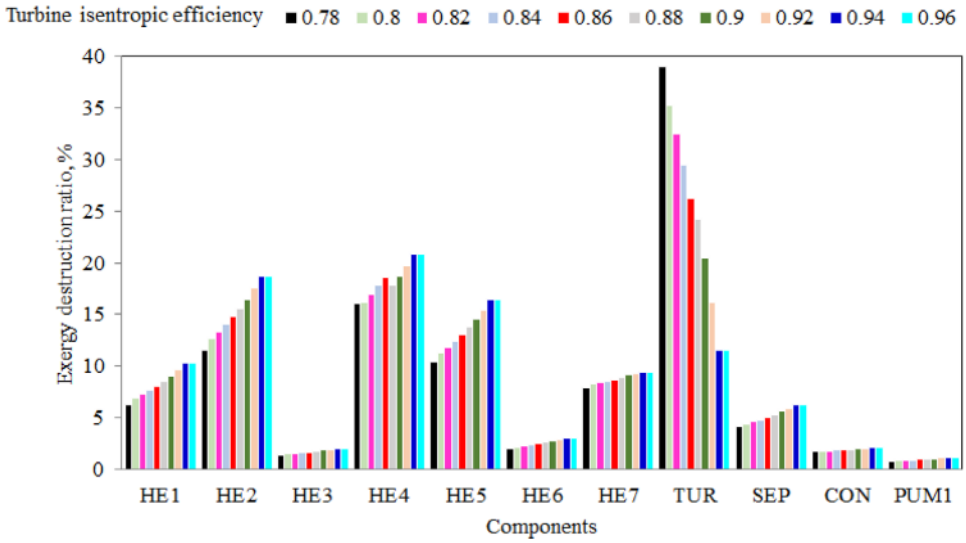


**FIGURE 8** Effect of isentropic efficiency on exergy destruction ratio

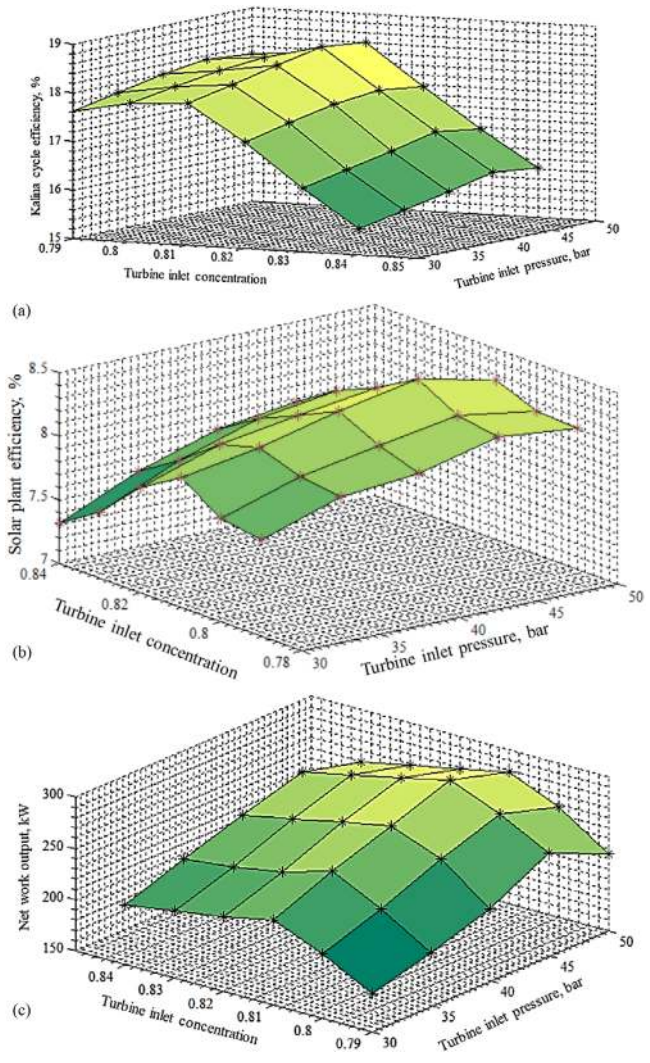


**FIGURE 9** Variation of (a) Kalina cycle efficiency, (b) solar plant efficiency and (c) net work output with turbine inlet temperature and turbine inlet pressure

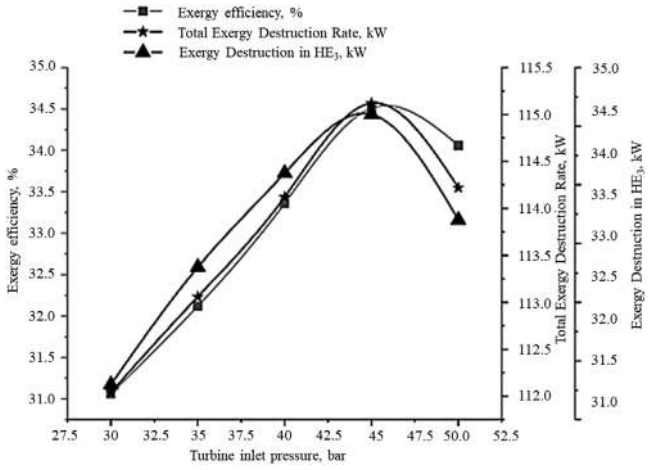


**FIGURE 10** Variation of exergy efficiency, net work output, total exergy destruction rate and $HE_3$ exergy destruction with pinch point temperature difference at $HE_3$

destruction rate increases with the combined changes in fuel and product exergy values.

The exergy values and cost rate of component state points at a fixed turbine inlet concentration and isentropic efficiency are summarised in Table 4. The total exergy is evaluated as the summation of physical and chemical exergy values of individual components. The unknown values of pressure, temperature and concentration of ammonia-water mixture were evaluated using energy and exergy balances. The temperatures at the turbine and pump exits were derived from the enthalpy and entropy values. The cost rate per unit exergy is necessary for evaluating the fuel and product exergy in assessing the exergy destruction rate of the cycle components.

In the conventional exergy analysis, the exergoeconomic parameters for the proposed system at 0.80 turbine inlet concentration and isentropic efficiency of 0.96 are summarised in Table 5. The components $P_2$ and $HE_5$ have lower operating

**TABLE 4** Energy, exergy and exergoeconomic properties of the cycle at 0.80 turbine inlet concentration, isentropic efficiency of the turbine as 0.96

| State | $P$ (bar) | $X$ | $T$ (°C) | $m$ (kg/s) | $h$ (kJ/kg) | $s$(kJ/kg K | Exergy ($Ex$), (kW) | $\dot{C}$ ($/hr) | $c$ ($/GJ) |
|---|---|---|---|---|---|---|---|---|---|
| 1 | 45 | 0.8 | 190 | 1.48 | 1825.3 | 5.05 | 24,119 | 2,806,728.03 | 320.40 |
| 2 | 12.03 | 0.8 | 118.4 | 1.48 | 1601.1 | 5.07 | 23,775 | 2,766,969.22 | 315.86 |
| 3 | 12.03 | 0.8 | 78 | 1.48 | 1024.6 | 3.55 | 23,592 | 2,724,303.35 | 310.99 |
| 4 | 12.03 | 0.98 | 78 | 0.98 | 1438.1 | 4.73 | 19,143 | 2,211,207.93 | 252.42 |
| 5 | 12.03 | 0.45 | 78 | 0.5 | 114.2 | 0.96 | 4442 | 514,566.51 | 58.74 |
| 6 | 12.03 | 0.45 | 78 | 0.02 | 114.2 | 0.96 | 166.1 | 15,957.94 | 1.82 |
| 7 | 12.03 | 0.45 | 78 | 0.48 | 114.2 | 0.96 | 4275.9 | 498,608.57 | 56.92 |
| 8 | 12.03 | 0.97 | 71.82 | 1 | 1453.1 | 4.77 | 19,312 | 2,101,084 | 239.85 |
| 9 | 12.03 | 0.97 | 74.24 | 1 | 1394.6 | 4.71 | 19,275 | 1,920,875.64 | 219.28 |
| 10 | 12.03 | 0.97 | 32 | 1 | 129.6 | 0.53 | 19,255 | 1,918,548.24 | 219.01 |
| 11 | 45 | 0.97 | 33.2 | 1 | 136 | 0.54 | 19,260 | 2,242,063.24 | 255.94 |
| 12 | 45 | 0.97 | 36.96 | 1 | 154.6 | 0.6 | 19,261 | 2,428,983.97 | 277.28 |
| 13 | 45 | 0.97 | 70.8 | 1 | 326.7 | 1.13 | 19,277 | 2,431,151.55 | 277.53 |
| 14 | 45 | 0.97 | 70.8 | 0.83 | 326.7 | 1.13 | 16,055 | 2,024,088.86 | 231.06 |
| 15 | 45 | 0.97 | 70.8 | 0.16 | 326.7 | 1.13 | 3221.4 | 353,431.76 | 40.35 |
| 16 | 45 | 0.97 | 108.4 | 0.16 | 1355 | 3.96 | 3251.9 | 357,541.28 | 40.82 |
| 17 | 45 | 0.97 | 108.4 | 0.83 | 1355 | 3.96 | 16,208 | 2,335,572.80 | 266.62 |
| 18 | 45 | 0.97 | 108.4 | 1 | 1355 | 3.96 | 19,460 | 2,139,596.39 | 244.25 |
| 19 | 45 | 0.8 | 108.4 | 1.48 | 782 | 2.58 | 23,663 | 2,638,950.43 | 301.25 |
| 20 | 45 | 0.8 | 129.22 | 1.48 | 1133.4 | 3.46 | 23,794 | 2,652,934.99 | 302.85 |
| 21 | 45 | 0.8 | 177.81 | 1.48 | 1787 | 4.96 | 24,100 | 2,685,082.22 | 306.52 |
| 22 | 45 | 0.45 | 77.8 | 0.48 | 114.7 | 0.95 | 4277.5 | 499,354.04 | 57.00 |

and maintenance costs. At the proposed parametric conditions, the exergoeconomic factor $f_i$ of the turbine is higher among the other components. The turbine exhibits a low exergetic efficiency among the major components of the system. The relative cost difference $r_i$ is highest for the components $HE_5$ and $P_2$. The investment cost functions of the separator and mixing chamber were not considered.

**TABLE 5** Individual component exergoeconomic factors and cost rates of proposed cycle 0.80 turbine inlet concentration, isentropic efficiency of turbine as 0.96

| Component | $\dot{E}_{D,i}$ (kW) | $\eta_{ex\ I}$ (%) | $Y_{D,I}$ (%) | $\dot{Z}_{D,I}$ ($/hr) | $r_{i(\%)}$ | $\dot{C}_{D,i}$($/hr) | $f_i$ (%) |
|---|---|---|---|---|---|---|---|
| MXT | 30.55 | 75.53 | 28.22 | 4.20 | 0.62 | 0.30 | 95.34 |
| $HE_1$ | 11.00 | 92.25 | 2.24 | 0.10 | 0.99 | 0.14 | 57.98 |
| $HE_2$ | 15.84 | 95.07 | 3.60 | 0.21 | 0.16 | 0.002 | 99.34 |
| $HE_3$ | 1.92 | 90.82 | 1.32 | 0.06 | 0.99 | 0.02 | 72.6 |
| $HE_4$ | 30.00 | 83.60 | 5.98 | 0.55 | 0.88 | 0.001 | 99.7 |
| $HE_5$ | 0.00 | 100 | 7.8 | 0.04 | 0.04 | 0.00 | 100 |
| $HE_6$ | 3.73 | 81.09 | 2.74 | 0.08 | 0.34 | 76.72 | 0.07 |
| $HE_7$ | 10.76 | 73.92 | 2.27 | 0.03 | 0.35 | 0.108 | 35.53 |
| CND | 7.00 | 92.25 | 6.95 | 0.15 | 0.59 | 0.09 | 59.77 |
| $P_1$ | 33.10 | 69.93 | 1.36 | 0.02 | 0.99 | 1.13 | 2.58 |
| $P_2$ | 0.00 | 99.95 | 0.00 | 0.01 | 0.21 | 0.00 | 100 |
| SEP | 7.00 | 99.97 | 20.95 | 0.00 | 0.0008 | 0.98 | 0.00 |
| $M_1$ | 33.4 | 99.82 | 8.65 | 0.00 | 0.05 | 0.001 | 0.00 |
| $M_2$ | 74.5 | 100.00 | 0.00 | 0.00 | 0.23 | 0.035 | 0.00 |
| $M_3$ | 0.00 | 99.9 | 7.91 | 0.00 | 0.01 | 0.01 | 0.00 |

## 5 | CONCLUSION

In this work, a novel Kalina power generation system was assessed for performance improvement in energy and exergy perspectives. The proposed novel Kalina power generation system is an improved design suitable for medium-temperature heat recovery applications with an additional solar collector. The design variables that were focused on system performance are the turbine inlet concentration, turbine inlet pressure, $HE_4$ outlet temperature from the turbine, condenser concentration of ammonia, isentropic efficiency of the turbine and pressure ratio. With the optimum design variables, the energy and exergy performances of the system were evaluated. Increasing the turbine inlet pressure to its optimum value, the cycle performance improves. The peak cycle performance includes 18.51% of KC efficiency, 8.28% solar plant efficiency, 34.51% exergy efficiency and 295.24 kW of net work output with the proposed design variables. A low pressure ratio yields higher energy performance of the novel system. The exergy destruction of the

major and minor components of the proposed system are at the turbine and mixing chamber. Opportunities have been identified for energy improvements and exergy destructions of this plant operating in a solar energy cascade. The present system has an increased flow rate at the turbine inlet with the parallel heat exchangers suing the recirculation of a portion of the lean liquid separated from the separator. With the additional solar concentrator arrangement, the required energy input to the system was reduced, which resulted in improved overall performance.

## ACKNOWLEDGEMENT

The authors confirm the development of a new design titled 'Thermodynamic cycle-based power generation system and a method', Application No.201741046830 A. We thank the financial support received from the management of Kingston Engineering College, Vellore, to execute this work.

## NOMENCLATURE

### Symbols

| | |
|---|---|
| $m$ | mass flow rate, kg/s |
| $h$ | specific enthalpy, kg/kJ |
| $x$ | mass fraction of ammonia, kg/kg mixture |
| $M$ | mechanical |
| $Q$ | heat supplied, kW |
| $I$ | irreversibility, kJ.kg K |
| $E$ | exergy, kJ |
| $MXT$ | mixture turbine |
| $F$ | vapour fraction |
| $M$ | mixing chamber |
| $Y$ | exergy destruction ratio, % |
| $N$ | annual unit operation hours |
| $\dot{Z}$ | Investment cost rate of components ($/hr) |
| $LMTD$ | logarithmic mean temperature difference (K) |
| $Z$ | investment cost of components ($) |
| $U$ | overall heat transfer coefficient (kW/m$^2$°C) |
| TTD | terminal temperature difference |
| $T$ | temperature, K |
| $W$ | work output, kW |
| $G$ | generator |
| $P$ | pressure, bar |
| $s$ | specific entropy, kJ/kg K |
| $ex$ | specific exergy, kJ.kg |
| $\dot{E}x$ | exergy rate, kW |
| HE | heat exchanger |
| SEP | separator |
| $S$ | separator |
| $C$ | cost rate ($/h) |
| CRF | capital recovery factor |
| $r$ | relative cost difference (%) |
| CND | condenser |
| $0$ | environment condition |
| $R$ | solar radiation, W/m$^2$ |

### Subscripts

| | |
|---|---|
| $KC$ | Kalina cycle |
| $ch,i$ | chemical, individual |
| $S$ | supply |
| $V$ | vapour |
| $cwin$ | cooling water inlet |
| $D$ | destruction |
| $P$ | product |
| $CI$ | capital investment |
| $C$ | specific exergy cost ($/GJ) |
| $Q$ | specific heat kJ/kg |
| $g$ | global |
| $ph,i$ | physical, individual |
| $P$ | pump |
| $l$ | liquid |
| $cwout$ | cooling water outlet |
| $F$ | fuel |
| tot | total |
| OM | operating maintenance |
| $w$ | specific work kJ/kg |
| $R$ | reference cost |

### Greek symbols

| | |
|---|---|
| $\eta$ | efficiency |
| $\varphi$ | maintenance factor |
| $\varepsilon$ | exergetic efficiency, % |

### Superscripts

| | |
|---|---|
| AV | avoidable |
| EN | endogenous |
| UN | unavoidable |
| CH | chemical |
| EX | exogenous |

## ORCID

*Narayanan Shankar Ganesh* https://orcid.org/0000-0002-2159-8369

## REFERENCES

1. Parikhani, T., et al.: Thermodynamic and thermoeconomic analysis of a novel ammonia-water mixture combined cooling, heating, and power (CCHP) cycle. Renewable Energy 145, 1158–1175 (2020)
2. Ghaebi, H., et al.: Exergoeconomic optimization of a novel cascade Kalina/Kalina cycle using geothermal heat source and LNG cold energy recovery. J. Cleaner Prod. 189, 279–296 (2018)
3. Ghaebi, H., et al.: Thermodynamic and thermoeconomic analysis and optimization of a novel combined cooling and power (CCP) cycle by integrating of ejector refrigeration and Kalina cycles. Energy 139, 262–276 (2017)
4. Ghaebi, H., et al.: Proposal and assessment of a novel geothermal combined cooling and power cycle based on Kalina and ejector refrigeration cycles. Appl. Therm. Eng. 130, 767–781 (2018)
5. Dhahad, H., et al.: Thermodynamic and thermoeconomic analysis of innovative integration of Kalina and absorption refrigeration cycles for simultaneously cooling and power generation. Energy Convers. Manage. 203, 112241 (2020)
6. Mokarram, N.H., Mosaffa, A.H.: A comparative study and optimization of enhanced integrated geothermal flash and Kalina cycles: A thermoeconomic assessment. Energy 162, 111–125 (2018)

7. Singh, O.K., Kaushik, S.C.: Thermoeconomic evaluation and optimization of a Brayton–Rankine–Kalina combined triple power cycle. Energy Convers. Manage. 71, 32–42 (2013)
8. Ghaebi, H., Parikhani, T., Rostamzadeh, H.: Energy, exergy and thermoeconomic analysis of a novel combined cooling and power system using low-temperature heat source and LNG cold energy recovery. Energy Convers. Manage. 150, 678–692 (2017)
9. Sun, F., et al.: Energy–exergy analysis and optimization of the solar-boosted Kalina cycle system 11 (KCS-11). Renewable Energy 66, 268–279 (2014)
10. Abdolalipouradl, M., et al.: Exergoeconomic analysis of a novel integrated transcritical CO2 and Kalina 11 cycles from Sabalan geothermal power plant. Energy Convers. Manage. 195, 420–435 (2019)
11. Mehrpooya, M., Mousavi, S.A.: Advanced exergoeconomic assessment of a solar-driven Kalina cycle. Energy Convers. Manage. 178, 78–91 (2018)
12. Shokati, N., Ranjbar, F., Yari, M.: A comprehensive exergoeconomic analysis of absorption power and cooling cogeneration cycles based on Kalina, part 1: Simulation. Energy Convers. Manage. 158, 437–459 (2018)
13. Sun, W., Yue, X., Wang, Y.: Exergy efficiency analysis of ORC (organic Rankine cycle) and ORC-based combined cycles driven by low-temperature waste heat. Energy Convers. Manage. 135, 63–73 (2017)
14. Vatani, A., Mehrpooya, M., Palizdar, A.: Advanced exergetic analysis of five natural gas liquefaction processes. Energy Convers. Manage. 78, 720–737 (2014)
15. Fiaschi, D., et al.: Exergoeconomic analysis and comparison between ORC and Kalina cycles to exploit low and medium-high temperature heat from two different geothermal sites. Energy Convers. Manage. 154, 503–516 (2017)
16. Rashidi, J., Yoo, C.K.: Exergetic and exergoeconomic studies of two highly efficient power-cooling cogeneration systems based on the Kalina and absorption refrigeration cycles. Appl. Therm. Eng. 124, 1023–1037 (2017)
17. Mahmoudi, S.M.S., et al.: Exergoeconomic evaluation and optimization of a novel combined augmented Kalina cycle/gas turbine-modular helium reactor. Appl. Therm. Eng. 109, 109–120 (2016)
18. Maheswari, G.U., Shankar Ganesh, N.: Performance investigation in modified and improved augmented power generation Kalina cycle using Python. Int. J. Energy Res. 44(3), 1506–1518 (2020)
19. Ganesh, N.S., Srinivas, T.: Power augmentation in a Kalina Power System for a Medium temperature low grade heat. ASME J. Sol. Energy Eng. 135(3), 1–10 (2013)
20. Shankar Ganesh, N., Srinivas, T.: Development of thermo-physical properties of aqua ammonia for Kalina cycle system. Int. J. Mater. Prod. Technol. 55(1/2/3), 113–141 (2017)
21. Shankar Ganesh, N., Srinivas, T.: Design and modeling of low temperature solar thermal power station. Appl. Energy 91(1), 180–186 (2012)
22. Mohammadi, A., et al.: Thermoeconomic analysis and multiobjective optimization of a combined gas turbine, steam, and organic Rankine cycle. Energy Sci. Eng. 6(5), 506–522 (2018)
23. Bejan, A., Tsataronis, G., Moran, M.: Thermal Design and Optimization. John Wiley & Sons, New York, USA (1996)
24. Chen, Y., et al.: Energy and exergy analysis of integrated system of ammonia–water Kalina–Rankine cycle. Energy 90, 2028–2037 (2015)
25. Wang, N., et al.: Thermodynamic performance analysis a power and cooling generation system based on geothermal flash, organic Rankine cycles, and ejector refrigeration cycle; application of zeotropic mixtures. Sustainable Energy Technol. Assess. 40, 100749 (2020)
26. Marston, C.H.: Parametric analysis of Kalina cycle. ASME J. Eng. Gas Turbines Power 112(1), 107–116 (1996)
27. Uysal, C.: A new approach to advanced exergoeconomic analysis: The unit cost of entropy generation. Environ. Prog. Sustainable Energy 39(1), e13297 (2019)
28. Chen, J., Havtun, H., Palm, B.: Conventional and advanced exergy analysis of an ejector refrigeration system. Appl. Energy 144, 139–151 (2015)
29. Ambriz-Díaz, V.M., et al.: Advanced exergy and exergoeconomic analysis for a polygeneration plant operating in geothermal cascade. Energy Convers. Manage. 203, 112227 (2020)
30. Montazerinejad, H., Ahmadi, P., Montazerinejad, Z.: Advanced exergy, exergo-economic and exrgo-environmental analyses of a solar based trigeneration energy system. Appl. Therm. Eng. 152, 666–685 (2019)
31. Mohammadi, Z., Fallah, M., Seyed Mahmoudi, S.M.: Advanced exergy analysis of recompression supercritical CO2 cycle. Energy 178, 631–643 (2019)


**How to cite this article:** Ganesh, N.S., et al.: Performance assessment of a novel power generation system. IET Renew. Power Gener. 15, 2205–2215 (2021). https://doi.org/10.1049/rpg2.12155